CHAPTER-4

Enhanced Ammonia Sensing with Au doped P3HT based Low-Voltage Operated Organic TFT on Bi-layer (TiO_2/HfO_2) Dielectric Film

The part of the work is adopted from-

A. Verma, V. N. Mishra, and R. Prakash, "**Self-Assembled Au/P3HT, High-k Bilayer Dielectric-Based Solution Processed Low Voltage OTFT for Multiparametric Ammonia Sensor at Room Temperature**," ***IEEE Transactions on Electron Devices*****,** vol. 70, no. 1, pp. 281-287, Jan. 2023, ***doi: 10.1109/TED.2022.3224092***.

Abstract:

A self-assembled, fully solution-processed, bilayer (TiO_2/HfO_2) dielectric-based thin film transistor (TFT) has been fabricated and explored for highly sensitive ammonia gas at room temperature (RT- 25 °C). The bilayer dielectric film has been grown over a heavily boron-doped Silicon substrate (p^{++} Si), and the thickness of each layer has been optimized by spin coating rotation speed and spin time to find a high-quality gate oxide. The obtained dielectric has a high areal capacitance of 0.926 μF/cm^2, low RMS roughness of 0.914 nm, and low leakage current density of ~1 μA/cm^2, high dielectric constant of ~42, which are much more favorable for the high-performance organic TFT. The incorporation of the TiO_2 layer in be-tween the p^{++} Si and HfO_2 layer enhances the areal capacitance and minimizes the RMS roughness (TiO_2 minimizes the no. of interface trap states at the dielectric/semiconductor interface) of the bilayer dielectric film, thereby improving the charge transfer mechanism. The developed high-k bilayer solution-processed dielectric layer has been utilized to develop a low voltage operated (-1.5 V) organic TFT for ammonia (NH_3) gas at RT. The fabricated OTFT device utilized the solution-processed floating film transfer method (FTM) to grow the Au(gold) doped P3HT film as a sensing/organic semiconductor channel (OSC) layer. The Au/P3HT sensing layer shows a quick response/recovery time (5/17 sec.), with a high sens-ing response of 55 % (5 ppm) towards the NH_3 analyte. The study aims to find a low-voltage, solution-processed, cost-efficient organic TFT device for a high-performance gas sensor at RT.

4.1 Introduction

IN recent days, the research community has very much potential attention over the

development of high-k (dielectric constant) based TFT (thin-film transistor) for various electronic applications [177], [182], [183]. These TFTs have potential applications in the era of memory devices, organic LEDs, flexible displays, gas sensors, and many more [182].

Although the conventional SiO_2-based TFTs passes with smooth surface roughness, defect-free oxide film, good oxide semiconductor interface, etc., it offers very low oxide capacitance (low k - 3.9) [41]. The oxide capacitance of the conventional SiO_2 film can be improved by minimizing the thickness of the SiO_2 film, as the dielectric capacitance is inversely proportional to the thickness of the oxide film. But the SiO_2 film became very leaky below 10 nm thickness. The advantage of the high-k dielectrics as a gate oxide layer is that it offers high gate oxide capacitance ($Cox \propto \frac{K}{t_{OX}}$, where k- dielectric constant, t_{ox} – oxide thickness) even at the high dielectric thickness and, therefore, reduces the operating potential of the TFTs below |2 V|, advantageous for low voltage and portable electronic circuits. A suitable high-k dielectric material must pass with the following properties: (1)- It's dielectric constant (k) should be in the range of 10 - 30 and have a large free Gibbs energy (0 to -50 KJ/mol favorable) (2)- The dielectric/oxide materials must be a good insulator (Band Gap $E_g > 5$ eV), and there will be a sufficient band offset between Si (Silicon) and dielectric interface ($E_{offset} > 1$ eV.) (3) good interface quality between oxide/semiconductor interface, low trap charge density ($< 10^{11}/cm^2$-eV.) [38], [39]. As compared to conventional SiO_2, the problem with the high-k dielectric/oxide materials is that they are extremely prone to charge traps due to defect formation with oxygen vacancies, poor RMS surface roughness, lower band offset, etc. these problems lead to a higher threshold voltage, lower device mobility and increase the leakage current of the fabricated devices. These problems can be overcome by using either a suitable

hybrid bilayer dielectric stack, dielectric composites, or organic-inorganic hybrid dielectric stack as a gate oxide material [41][184].

In the present work, a bilayer solution-processed gate oxide stack of TiO_2 (titanium dioxide) and HfO_2 (hafnium oxide) has been synthesized for low voltage operated solution-processed organic thin film transistor (OTFT) for highly sensitive NH_3 gas at RT (25 °C). The incorporation of the TiO_2 layer in between the HfO_2 and p^{++} Si interface makes a Schottky junction (electron easily travels from n-TiO_2 to p^{++} Si and offers a large barrier height for hole travels from p^{++} Si to n-TiO_2 at 0 V gate bias (fermi level alignment)), induces positive charge at semiconductor/dielectric interface that reduces the interface trap states, subthreshold swing (SS) and improves the OTFT performance [185][186] (possible mechanism has been explained in **Section (4.4.4)**). The developed dielectric with an optimized thickness of the TiO_2 layer and HfO_2 layer offers high areal capacitance, low leakage current density, low RMS surface roughness (reduces carrier scattering and improves mobility), etc., which is favorable for device performance and sensing application. The current work has a potential application for NH_3 sensing at room temperature (RT-25 °C). NH_3, emanating from industrial applications, crude oil extraction, agricultural lands, refineries, etc., is a highly toxic, combustible, and colorless gas with a pungent smell [16][187]. This irritating pungent smell gas has a safety standard of 35 ppm for 15 minutes by OHSA (occupational safety and health) [105]. Over the defined limit given by OHSA, this dangerous gas may cause lung damage, blindness, coma, collapse, seizures, and death [16][105]. So, it is important to develop an efficient and highly selective NH_3 gas sensor that can prevent fatal accidents and life-threatening issues. In this work, Au nanoparticle-doped P3HT nanocomposite as an active/sensing layer

has been developed by a cost-efficient solution-processed FTM (floating film transfer method) on developed HMDS vapor phase treated bilayer dielectric film possible for the first time. The current work aims to fabricate a cost-efficient, low-voltage operated solution processed OTFT for various electronic applications.

4.2 Experimental Section

4.2.1. Chemicals Required and Material Synthesis

P3HT (Poly(3-hexylthiophene-2,5-diyl) (MW 50k -75k) was procured from Sigma Aldrich Pvt. Ltd. Titanium isopropoxide (TTIP) ($C_{12}H_{28}O_4Ti$), Hafnium chloride ($HfCl_4$), Chloroform ($CHCl_3$), 2 Methoxy ethanol (2ME), Hexamethyldisilazane (HMDS), Isopropanol (C_3H_8O), Ethanol, Hellmanex™ III was procured from Merck India Pvt. Ltd.

A 100 mM of TTIP and $HfCl_4$ were prepared separately in 2 ME, and the solution was kept on constant stirring at 900 rpm, 40 ºC for 5 hours to form a clear transparent solution and filtered by a 0.22 um pore size PTFE syringe filter to remove unwanted large particles. The solution for the active layer (Au/P3HT) has been prepared with 5 mg of P3HT polymer in 1 ml $CHCl_3$ solvent and 3 mg/ml $AuCl_3$ in an ethanol solution separately. The Au solution was doped in P3HT solution and optimized to form a 0.1% wt/wt active layer solution[188]. Further, the active layer solution was kept on constant stirring at 900 rpm at RT (25 °C) for 90 minutes to form a clear, uniform solution. A cost-efficient, minimal wastage, simple FTM method has been adopted to grow the organic semiconductive channel (OSC) layer. The steps to be followed for the FTM method have been demonstrated in the article-[16] [178].

4.2.2. Device Fabrication

The subsequent steps to be followed for the fabrication of this device has been given as follows. The highly doped p^{++} boron-doped silicon was cleaned ultrasonically in 1% Hellmanex

III in warm DI water for 10 minutes. Further, the substrate was dipped in isopropanol for 5 minutes and rinsed with running DI water. The substrate was dipped in piranha solution (H_2O_2: H_2SO_4 = 6:4)) for 20 minutes, followed by rinsing in running DI water. The 15% HF solution in DI water treatment has been used to etch out the native oxide film from the substrate surface, subsequently rinsed in running DI water several times and baked in N_2 ambient to eliminate the DI water droplets from the Si substrate. The plasma treatment was done for 15 minutes for surface activation and eliminated the hydroxyl ion (-OH-) from the substrate surface. The plasma treatment substrate forms hydrophilic, free from pinholes, and has an excellent adhesive-cleaned surface. The TTIP in 2ME solution was spin-cast on cleaned plasma treated p^{++} Si at 6000 rpm for 60 sec. The TTIP solution-coated substrate was pre-annealed for 10 minutes at 90 ºC, followed by high-temperature annealing at 350 ºC in N_2 ambient for 40 minutes to develop a thin TiO_2 dielectric layer. After that, on top of this, $HfCl_4$ in the 2ME solution was spin-cast with a 6000 rpm speed for 60 sec. followed by pre-annealing at 90 ºC to evaporate the solvent. Further, $HfCl_4$ coated substrate was post-annealed at 500 ºC for 40 minutes in N_2 ambient to form TiO_2/HfO_2 bilayer dielectric film. The obtained bilayer dielectric film was treated with the vapor phase HMDS method for 20 minutes to obtain a thin SAM (self-assembled monolayer) hydrophobic substrate [189]. Subsequently, the OSC layer was deposited by the FTM method [16][187], followed by annealing at 80 ºC for 60 minutes to remove the residue of organic solvent. The obtained OSC film thickness was 30±5 nm measured by Filmetrics F20-UV. A 55 nm gold interdigitated source/drain contact of 18 mm/50 um channel width/length was deposited by thermal evaporation unit HHV B12A4D at a constant pressure of 2×10^{-6} torr. **Figure 4.1(a)** and **Figure 4.1(b)** show

the device illustrative diagram and a picture of the Organic TFT device, respectively.

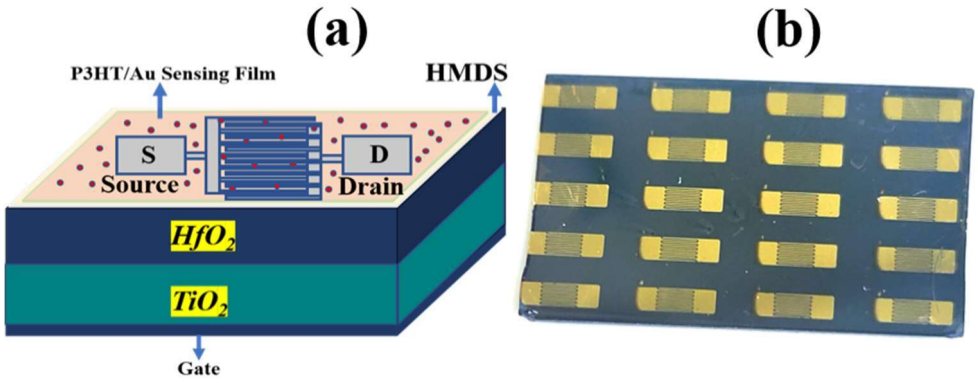

Figure 4.1 (a) Illustrative diagram of the device, (b) Picture of the fabricated organic TFT device.

4.3 Film Characterization and Sensing Setup

The X-ray diffraction (XRD) pattern of annealed single layer and bilayer dielectric (TiO_2/HfO_2) characterized by using Rigaku smart lab 9 KW equipped with Cu-Kα source has been plotted in **Figure 4.2(a)**. The TiO_2 (titanium dioxide) film annealed at 350 °C passes with diffraction peaks positioned at 24.91°, 37.45°, 47.86°, and 62.64° responsible for (101), (004), (200), and (213), respectively. The thin film TiO_2 on the Si substrate shows a sharp peak (101) at 24.91°[190][191]. The HfO_2 (hafnium oxide) annealed at 500 °C passes with diffraction peaks positioned at 24.17°, 28.07°, 31.52°, 34.48°, and 50.19° responsible for (001), (100), (111) and (002), and (220), respectively [192]. The XRD pattern of Au-doped P3HT polymer has a sharp diffraction peak at 5.87° (100) along with other secondary diffraction peaks at 11.07° (200),16.37°(300), 38.47°(111), 44.7°(200), respectively. The minor peaks at 38.47º(111) and 44.7º(200) are due to Au nanoparticles in the P3HT polymer matrix [193]. The tauc plot of the fabricated bilayer dielectric film and TiO_2 film have been plotted in **Figure 4.2(b)**. Although the single TiO_2 layer offers a high oxide/dielectric

capacitance (k value ~ 60 to 80) but has a low Eg (band gap) of 3.45 eV., which is not appropriate for a high-performance gate oxide material as it suffers from a large gate leakage current. On the other hand, over the single TiO_2 film, TiO_2/HfO_2 (bilayer dielectric) film passes with quite large band gap of 5.6 eV., sufficient to suppress the gate leakage current and passes with good oxide capacitance**.**

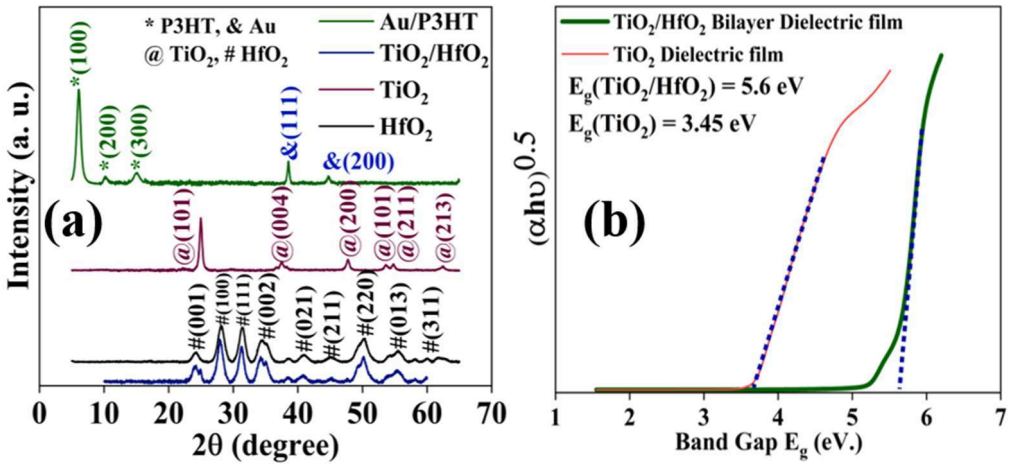

Figure 4.2 (a) X-ray diffraction pattern of Au/P3HT, TiO_2, HfO_2, and TiO_2/HfO_2 film, (b) Tuck plot of TiO_2 and TiO_2/HfO_2 film.

The surface morphologies of the single TiO_2, HfO_2, and bilayer dielectric film have been studied with the atomic force microscopy (AFM) (Model -NTEGRA Prima company- NT-MDT Service & Logistics Ltd.) plot shown in **Figure 4.3**. For a high-performing OTFT, the dielectric/oxide surface must pass with very low RMS roughness (smooth film), usually less than 1 nm. The AFM image of TiO_2 over the Si substrate has a very low RMS roughness of 0.253 nm (shown in **Figure 4.3(a)/(a')**), which is very less (almost 2.5 times) compared to the RMS roughness of HfO_2 over p^{++} Si substrate (indicated in **Figure 4.3(b)/(b')**). The low RMS roughness of the TiO_2 layer indicates the good interface properties of dielectric film over the silicon substrate. The low RMS roughness of TiO_2 over the Si substrate offers low

interface trap states, which minimize the charge carrier scattering, improve the carrier's mobility, reduce the voltage for charge accumulation, and enhance the charge transfer mechanism (The possible reason has been discussed in **Section (0)**)- Device physics and sensing mechanism). Here utilizing the TiO_2 thin film between p^{++} Si and HfO_2, the bilayer dielectric layer (TiO_2/HfO_2) passes with RMS roughness of 0.915 nm (refer to **Figure 4.3(c)/((c')**), which is quite favorable for the OTFT fabrication process.

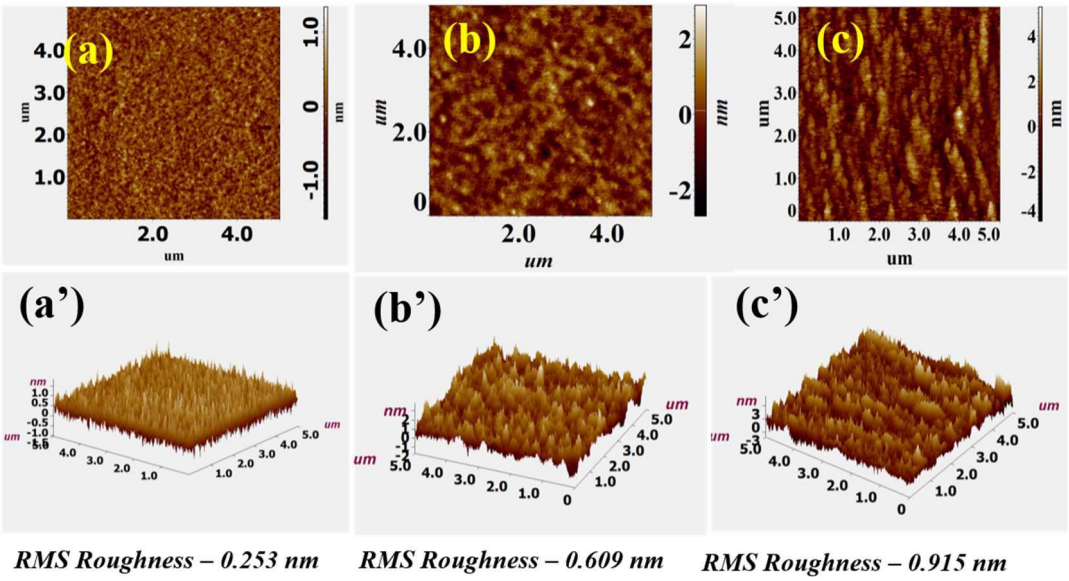

Figure 4.3 (a)/(a') 2D/3D AFM of TiO_2 film, (b)/(b') 2D/3D AFM image of HfO_2 film, (c)/(c') 2D/3D AFM of TiO_2/HfO_2 film.

The capacitance-voltage (C-V) plot and capacitance-frequency (C-f) plot of fabricated dielectric has been plotted in **Figure 4.4(a)** and **Figure 4.4(b)**, respectively. The CV plot in **Figure 4.4(a)** indicates the bilayer film has an ariel capacitance (C_{eff}) of 0.926 μF/cm^2 at -1.5 V, 1 kHz frequency. The C-f plot in **Figure 4.4(b)** compares the dielectric capacitance of the bilayer dielectric (TiO_2/HfO_2) with single-layer HfO_2 at almost the same dielectric film thickness. It has been observed that the fabricated bilayer dialectic with 40 nm thickness

offers more capacitance as compared to the HfO_2 layer (~46 nm (two coatings) measured by Filmetrics F20-UV). The high dielectric capacitance is obvious due to the high dielectric constant of the TiO_2/HfO_2 bilayer (k value ~42) film.

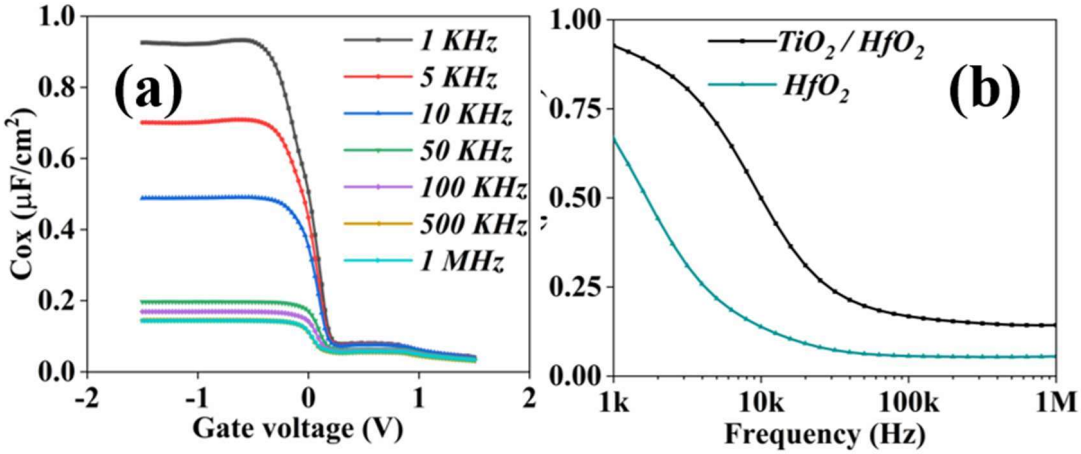

Figure 4.4 (a) Capacitance -voltage (C-V) plot of fabricated bilayer dielectric (TiO_2/HfO_2) film at -1.5 V, 1 kHz, (b) Capacitance -frequency (C-f) plot of fabricated bilayer dielectric (TiO_2/HfO_2) film and HfO_2 film at -1.5 V.

The thickness of each layer in bilayer dielectric film i. e. TiO_2 and HfO_2 film has been optimized to obtain high capacitance and suppress leakage current as compared to a single TiO_2 or HfO_2 layer. In work, the dielectric film thickness has been optimized with the spin coating rotation time and speed. The thickness of the synthesized dielectric has been observed by Filmetrics F20-UV at various points of 17± 3 nm 21± 4 nm for layer TiO_2 and HfO_2 over the p^{++} Si substrate, respectively. It is well known that TiO_2 over p^{++} Si film has a high dielectric constant and low surface RMS Roughness over HfO_2 on p^{++} Si substrate, but it has a very low dielectric band gap of 3.45 eV. (Indicated in the tauc plot in **Figure 4.2(b)**), which increases the gate leakage current of the dielectric film. On the other hand, HfO_2 minimizes the leakage current but has a low dielectric constant (k value 22), thereby reducing the areal oxide capacitance and current driving capability of the transistor. In this work, the advantage

of TiO_2 in terms of good interface properties, high oxide capacitance, and HfO_2 (High band gap ~ 5.8 eV) in terms of minimizing the leakage current has been utilized to develop an efficient gate oxide/dielectric material for OTFT device [194]. The leakage current density of the fabricated dielectric is ~1 μA/cm^2 at -6 V applied gate voltage (indicated in **Figure 4.5(a)**). The leakage current density plot in **Figure 4.5(a)** shows that the dielectric film can work in satisfactory conditions up to a -6 V supply. The effective capacitance (C_{eff}) of the bilayer dielectric film can be given by a parallel plate capacitor –

$$\frac{1}{C_{eff}} = \frac{1}{C_{TiO_2}} + \frac{1}{C_{HfO_2}} \tag{4.1}$$

Where C_{TiO2}, C_{HfO2} have been defined as $\frac{K_{TiO_2} * \varepsilon_0}{t_{TiO_2}}$, and $\frac{K_{HfO_2} * \varepsilon_0}{t_{HfO_2}}$, respectively. k, t are the respective dielectric constant and thickness of the dielectric film, respectively.

The average surface roughness of the OSC layer over the solution-processed dielectric film is 1.732 nm, and its AFM morphology is shown in **Figure 4.5(b)**. The high avg. surface roughness offers more reactive sites or a higher surface-to-volume ratio for gas molecules adsorption/desorption and incorporated in quick and high sensing response [195].

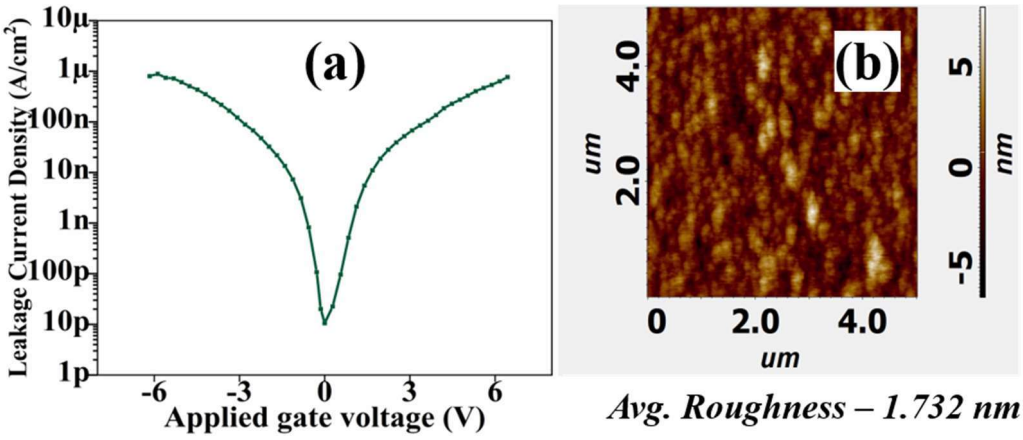

Figure 4.5 (a) Leakage current density plot of bilayer dielectric (Al/TiO_2/HfO_2/ Al) film, (b) AFM of Au/P3HT film over TiO_2/HfO_2/HMDS dielectric film.

The gas sensing measurement has been carried out by our indigenous sensing setup of a 10-liter chamber with a controlled mass flow controller (flow rate set to 10 ml/minute), humidity sensor, temperature sensor, semiconductor parameter analyzer Keysight B1500A, etc., shown in **Figure 4.6**. All the sensing characterization has been carried out at RT, ambient air, and 46 % relative humidity.

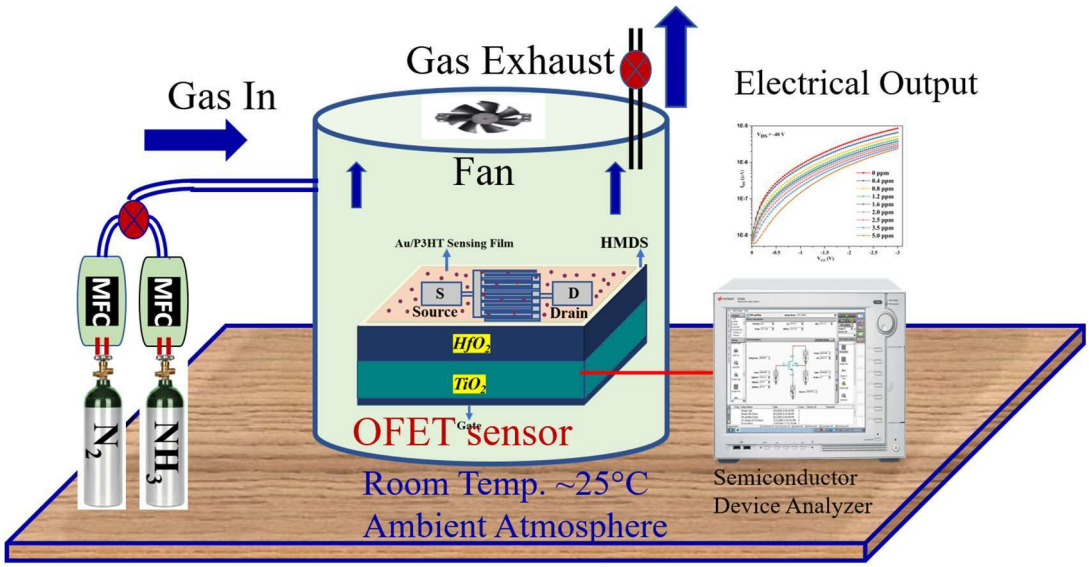

Figure 4.6 Illustrative schematic of the indigenous gas sensing setup.

4.4 Electrical, Sensing Results, and Discussion

4.4.1. Electrical Outputs

The I_{DS}- V_{DS} (drain curve plot), and I_{DS} -V_{GS} (transfer curve plot) for fabricated OTFT with sweep applied voltage of 0 to -1.5 V are indicated in **Figure 4.7(a)** and **Figure 4.7(b)**, respectively. The operating voltage (O. V.) of the TFT has been optimized with varying dielectric thickness for low voltage operation, low leakage current with high drain current. The curve demonstrates that the device obtained a good saturation current of -8.59 µA at -1.5 V V_{GS}, V_{DS} supply. The I_{DS} of the fabricated OTFT in the saturation region is given by [16].

$$I_{DS} = \mu_P C_{eff} \frac{W}{2L}(V_{GS} - V_{TH})^2 \; ; \; V_{DS} \geq V_{GS} - V_{TH} \tag{4.2}$$

Where μ_p – mobility, W/L – aspect ratio, V_{GS}, V_{DS} – gate to source and drain to source voltage, and V_{TH}- threshold voltage of the OTFT, respectively. The fabricated TFT has a μ_p of 0.1069 cm^2/V. sec., high I_{on}/I_{off} of ~10^3, and SS of 0.5094 V/decade, respectively.

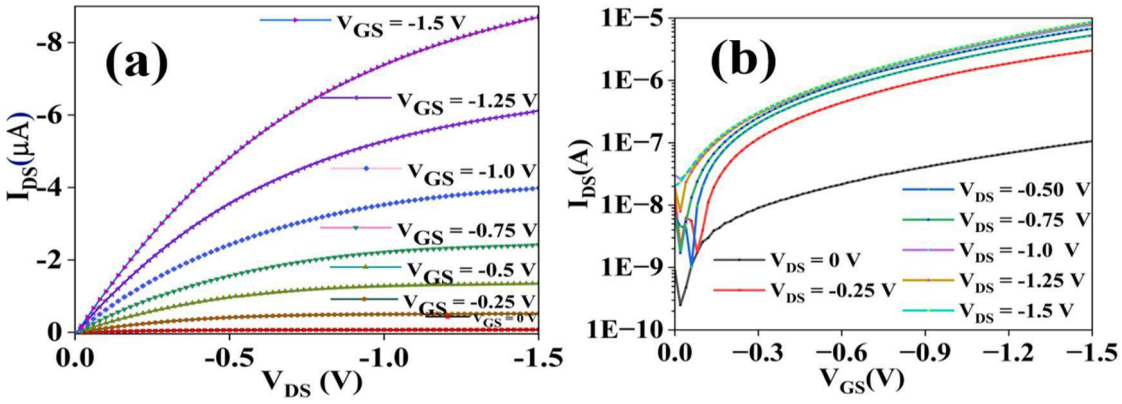

Figure 4.7 (a) I_{DS}-V_{DS} plot of the fabricated low voltage device, (b) I_{DS}-V_{GS} plot of the fabricated low voltage OTFT device.

4.4.2. Sensing Results

The fabricated solution process high-k-based OTFT has been utilized for NH_3 gas sensing. The sensing results have been taken on the transfer characteristics of the transistor due to its multi-parameter extraction in terms of mobility, threshold voltage, SS, trap charge, etc. The transfer curve plot for V_{GS} sweep from 0 to -1.5 V at -1.5 V, V_{DS} has been used for gas sensing experiment is shown in **Figure 4.9(a)**. The parameters can be calculated as follows.

4.4.2.1. Mobility, Threshold voltage, Subthreshold swing, Trap charge density with Exposed NH_3 Gas.

The parameters μ_p, V_{TH}, and SS of the fabricated transistor can be extracted graphically from the SQRT I_{DS} and log plot of $|I_{DS}|$, respectively. The square root of I_{DS} can be given as-[16]

$$\sqrt{I_{DS}} = \sqrt{\mu_P C_{eff} \frac{W}{2L}(V_{GS} - V_{TH})} = aV_{GS} - b \tag{4.3}$$

Mobility (μ_p) and threshold voltage (V_{TH}) can be calculated by-

$$\mu_P = \frac{2}{AR.C_{eff}}a^2 \qquad \& \qquad V_{TH} = \frac{-b}{a} \tag{4.4}$$

The subthreshold swing (SS)can be calculated by-[196]

$$SS = max\left|\left(\frac{\partial \log_{10}\left|I_{DS(V_{D,max})}\right|}{\partial V_G}\right)^{-1}\right| \tag{4.5}$$

The variation in the trapped charge (Q_{trap}) is highly responsible for gas sensing response can be defined as [16]

$$Q_{trap} = \Delta V_{TH} * C_{eff} \tag{4.6}$$

The extracted parameters with exposed NH_3 gas are given in **Table 4.1**. The shift in μ_p, V_{TH}, and trap charge with exposed varying NH_3 gas is plotted in **Figure 4.8(a)**. and **Figure 4.8(b)**, respectively. The sensing response S (%) and shift in threshold voltage (V_{TH}) plot with exposed NH_3 concentration is shown in **Figure 4.9(b)**. It has been observed that the exposed NH_3 gas traps the active charge carriers and reduces the drain current of the organic TFT.

Table 4.1 Extracted Parameters with Exposed NH_3 Analyte (0 to 5 ppm)

NH_3 (ppm)	$\|I_{on}\|$ (μA)	S (%)	μ_p (cm^2/V. Sec.)	V_{TH} (V)	SS (V/dec.)	Trap Charge (nQ/cm^2)
0	8.59	0.00	0.1069	-0.1539	0.5094	0
0.4	7.06	17.84	0.0907	-0.1778	0.5274	21.5
0.8	5.95	30.67	0.0830	-0.2071	0.5369	47.8
1.2	5.31	38.10	0.0780	-0.2594	0.5476	94.9
1.6	4.87	43.20	0.0738	-0.3204	0.5571	149.8
2	4.53	47.28	0.0709	-0.3683	0.5646	192.9
2.5	4.27	50.33	0.0680	-0.4048	0.5749	225.7
3.5	4.02	53.14	0.0660	-0.4372	0.5886	255.0
5	3.81	55.66	0.0627	-0.4980	0.6017	309.6

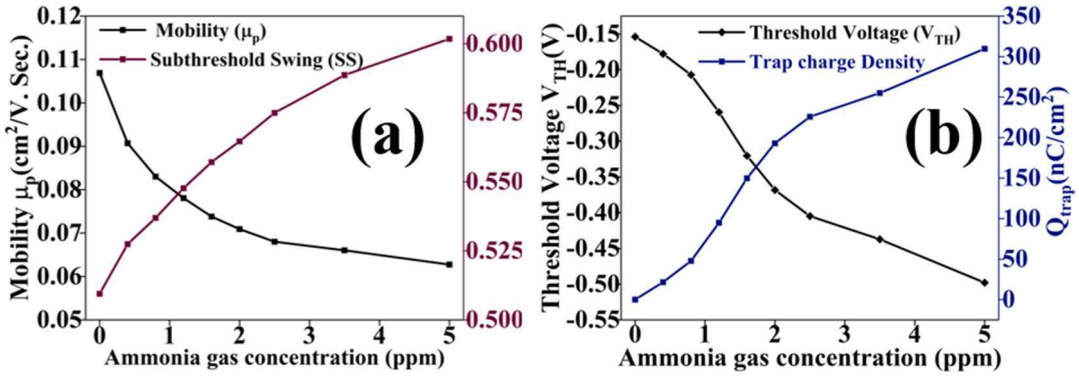

Figure 4.8 (a) Mobility (μ_p) and subthreshold swing (SS), (b) Threshold voltage (V_{TH}) and Q_{Trap}, with varying NH_3 concentration (0 to 5 ppm).

4.4.2.2. Sensing Response and Limit of Detection

The sensing response is a crucial parameter in defining the quality of the sensors. The sensing response can be defined as-.

$$S\% = \frac{\left|I_{DS(AIR)} - I_{DS(GAS)}\right|}{I_{DS(AIR)}} * 100\% \tag{4.7}$$

$I_{DS(AIR)}$ -Drain current in ambient Air, $I_{DS(GAS)}$ -Drain current in NH_3 gas. The fabricated sensor's detection limit (LOD) can be calculated graphically by extrapolation of the sensing response plot at a low concentration of the exposed analyte. The sensing response and LOD for the fabricated sensor are 55% at 5 ppm NH_3 gas and LOD of 15.15 ppb, respectively.

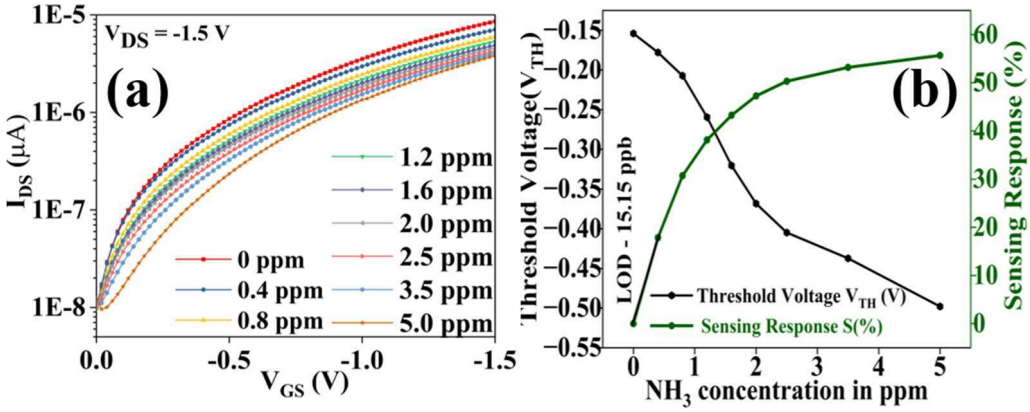

Figure 4.9 (a) Transfer curve plot of the transistor at varying NH_3 concentration (V_{DS}= -1.5 V), (b) Sensing response plot (at V_{GS} = V_{DS}= -1.5 V) and threshold voltage (V_{TH}) with varying NH_3 gas concentration.

4.4.2.3. Transient/Repetitive and Relative Humidity Analysis

To investigate the speed of the gas sensor, the transient analysis of the OTFT sensor has been shown in **Figure 4.10(a)**. The response/recovery time of the gas sensor is usually related to chemisorption (bulk mechanism) or physisorption mechanism (a surface mechanism) at the sensing surface. Here the fabricated sensor follows the dominant physisorption mechanism; thereby, the fabricated sensor has an average response ($T_{res.}$) and recovery time ($T_{rec.}$) of 6 and 17 sec., respectively. The vapor in the ambient air degrades the sensor's performance, so the humidity analysis is the most interfering effect for sensing devices, which is much more important to investigate the reliability of the sensor. Here in the present study, the humidity analysis has been carried out at 1.2 ppm and 0 ppm, plotted in **Figure 4.10(b)** and **Figure 4.10(c)** (inset fig.), respectively. The variation in relative humidity (RH) ranges from 30% to 70%, as shown in **Figure 4.10(b)** and **Figure 4.10(c)** clarifies that the sensor passes with a very minute change in sensing response of 4 to 5% with 30% to 70% of RH variation. The insensitive sensing response with the variation in the RH is probably attributed to the high crosslinking of Au nanoparticles in the polymer matrix, suppressing the diffusion of oxygen and moisture at the sensing surface [197].

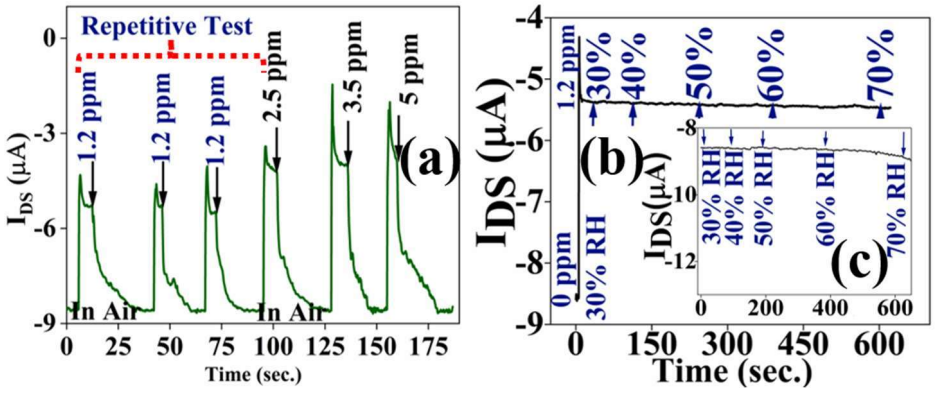

Figure 4.10 (a) Transient/repetitive response of fabricated OTFT sensor (at V_{GS}=V_{DS}= -1.5 V), (b) RH analysis over the I_{DS} vs. time plot at 1.2 ppm, (c) Effect of RH over the I_{DS} vs. time plot in air (variation range over 30% to 70% at V_{GS}=V_{DS}= -1.5 V).

4.4.2.4. Selectivity and Relative Stability

The investigation of the sensor's selective response towards ammonia gas and selectivity analysis of the fabricated sensor for various interfering gases (CO_2, CO, CH_4, propane, H_2) has been shown in **Figure 4.11(a)**. It can be said that the developed sensor is a promising candidate for ammonia gas sensing at RT. The device stability study over 4 weeks have been plotted in **Figure 4.11(b)**, shows a high level of relative stability, probably due to the metal nanoparticles crosslinking in the polymer matrix, making it insensitive to RH variation over a long time [197].

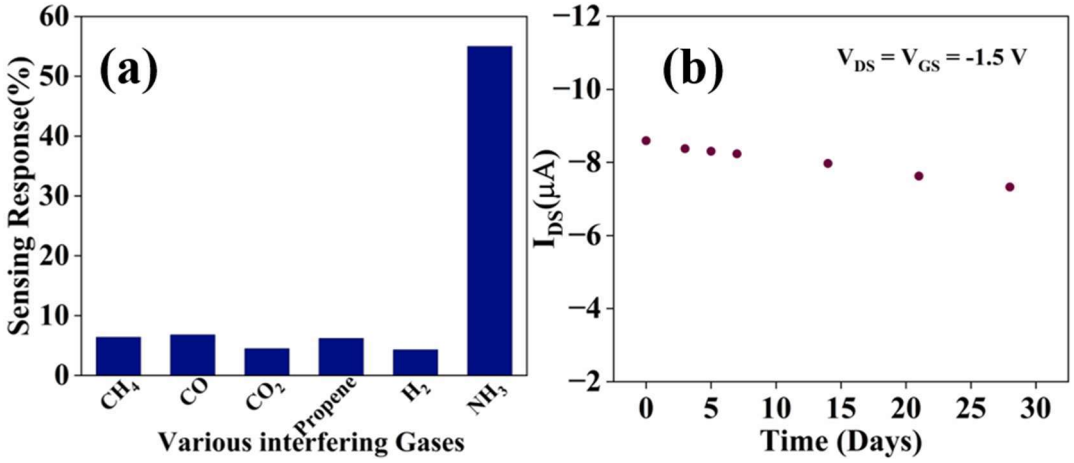

Figure 4.11 (a) Selectivity bar chart of the fabricated device over various interfering gases (CH_4, CO, CO_2, Propane, H_2 - 25 ppm, NH_3 -5 ppm), (b) Relative stability of the sensor over 4 weeks.

4.4.3. Comparative Analysis

The investigation of comparative analysis has been performed to check the quality of the sensor with respect to other already available sensors. The comparative **Table 4.2** explicates that the fabricated high-k bilayer dielectric-based OTFT with Au-doped P3HT film as an active layer has versatile applications in the field of ammonia sensing at RT.

Table 4.2 Comparative Analysis of the Fabricated Gas Sensor

Device Architecture	Sensing Material	Fabrication Method	S (%) (ppm)	O. V. /Temp.	$T_{res.}$ /$T_{rec.}$ (sec.)	Remarks [Ref.]
MSM	PQT -12	Spin coating	8 (100 ppm)	5 V/RT	8/103	Poor sensing response [124]
MSM	PANI/rGO	Drop Costing	11 (100 ppm)	-/RT	50/23.	Low response, response time [198]
Chemiresistive	rGO/ PAni	Drop Casting	2.8 (0.2 ppm)	-/25 °C	800/400	Poor response/recovery time [199]
Chemiresistive	WO_3	Spin Coating	5.11 (5 ppm)	-/250 °C	23/25	Poor sensing response [200]
OTFT	P3HT/MoS_2	FTM	63 (100 ppm)	-60 V/25 °C	-	Low sensing response/high operating voltage [16]
OTFT	PBTTT	FTM	89 (100 ppm)	-60 V/25 °C		Poor sensing response/high operating voltage [17]
TFT	Graphene	Spin coating	20 (3 ppm)	2 V/ 25 °C	40/120	Slightly low sensing response/ poor response, recovery time [177]
OTFT	Au/P3HT	FTM	55 (5 ppm)	-1.5V/25 °C		Low voltage operated/Fast response/recovery/high response [Our Work]

MSM- Metal Semiconductor Metal

4.4.4. Device Physics and Sensing Mechanism

This section briefly discusses the device physics and sensing mechanism for ammonia gas sensing. The utilization of the bilayer dielectric not only enhances the dielectric/oxide ariel capacitance but also suppresses the leakage current density of the dielectric layer. The bilayer dielectric combines the advantage of both single layers, TiO_2 in terms of high-k value (60 to 80) offers high ariel oxide capacitance, and HfO_2 (k value is 22) in terms of the high band gap of 5.6 eV. to suppress leakage current, and results in high current driving capability (I_{DS} α C_{eff}). The fabricated bilayer dielectric film offers low leakage current density of ~1 $\mu A/cm^2$ at -6 V, high areal oxide capacitance of 0.986 $\mu F/cm^2$ (at -1.5 V, 1 kHz), low dielectric film roughness of 0.915 nm (indicated in **Figure 4.3(c)/(c')**), these properties make it's as a potential candidate for the gate oxide in OTFT fabrication. **Figure 4.12(a)** explains the bilayer

dielectric (TiO_2/HfO_2), p^{++} Si interface mechanism responsible for smooth and good dielectric/semiconductor interface. The incorporation of the TiO_2 layer makes a Schottky contact and forms Ti-Silicide over p^{++} Si substrate [194]. The electrons from the n-TiO_2 easily travel to the p^{++} Si, which induces a positive charge at the HfO_2/Au/P3HT interface, thereby diminishing the required threshold voltage for the conduction process and also improving the RMS roughness of the dielectric surface [185][186]. The charge transfer mechanism from n-TiO_2 to the p^{++} Si region induces a positive charge at the semiconductor/HfO_2 interface, which minimizes the available trap charge states and requires low voltage for charge accumulation and conduction process for the device operation [185]. Over the bilayer dielectric, in the single layer HfO_2 over p^{++} Si, no charge transfer mechanism takes place between interface (offers high band offset ΔEc =2.7 eV., ΔEv =3.0 eV. over p^{++} Si [201]); thereby, the relatively more available trap states at the HfO_2/Au/P3HT interface requires relatively high threshold for charge accumulation and conduction process and also increases dielectric RMS roughness (indicated in **Figure 4.3(b)/(b')**). The low no. of available charge traps in the oxide interface region at 0 V gate bias and charge accumulation at negative gate bias is shown in **Figure 4.12(a)** and **Figure 4.12(b)**, respectively.

The gas sensing mechanism can be briefly described by the de-doping/doping interaction over the sensing surface when the analyte ammonia has been exposed [16][196]. As a reducing agent, each ammonia molecule has a tendency to donate its lone pair electron to the Au-doped P3HT sensing surface of the fabricated sensor. The ammonia molecules interact with the Au/P3HT sensing surface by donating its lone pair electrons and trap the active charge carriers (mainly responsible for the drain current), thereby deplete the OSC. The continuous

depletion or trapping of the active charge carriers across the channel upon the exposure of ammonia analyte modulates (reduces) the drain current of the fabricated solution processed OTFT device, and incorporate in the sensing phenomenon of the sensor. The trapping charge over the sensing surface creates an additional LUMO (lowest unoccupied molecular orbital) level in the Au/P3HT matrix, which reduces the drain current of the TFT [16]. The trapping of the active charge carrier with exposed ammonia analyte has been illustrated in **Figure 4.12(c)**.

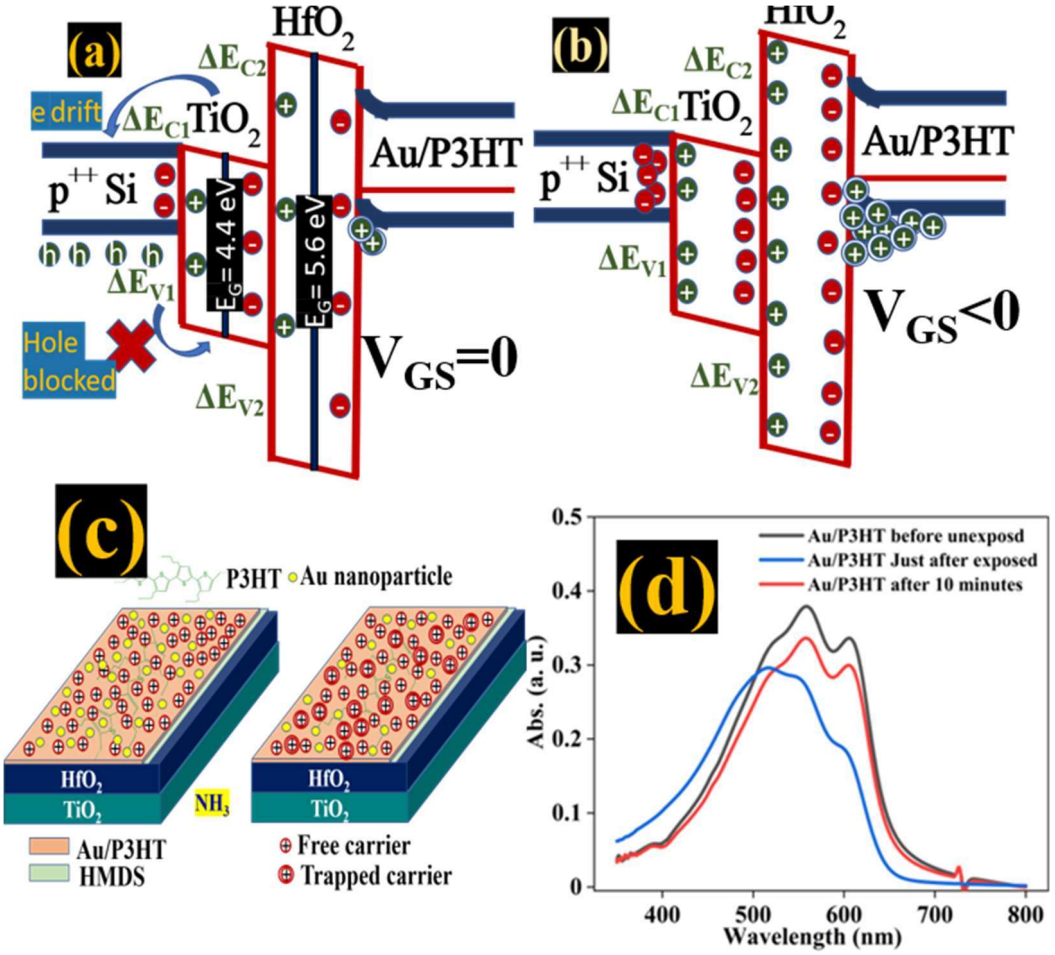

Figure 4.12 (a) Dielectric/semiconductor interface of p^{++}Si and TiO_2/HfO_2/Au/P3HT film at 0 V gate bias, (b) Dielectric/semiconductor interface of p^{++}Si and TiO_2/HfO_2/Au/P3HT film at negative gate bias, (c) Charge trapping mechanism over the Au/P3HT sensing film upon NH_3 exposed, (d) NH_3 interaction mechanism with the sensing film by UV-Vis. spectroscopy.

In order to validate the interaction mechanism of NH_3 over the sensing film UV. Vis. Spectra has been recorded in **Figure 4.12(d)**. The adsorption of the ammonia molecule over the Au/P3HT sensing surface shifts the main absorption peak to 515.6 nm from 560.6 nm with reduced absorption intensity. The broadening and shifting of the peak are due to the formation of Au/P3HT/NH_3 charge complexes over the sensing surface shown in **Figure 4.12(c)**. when the gas ambient has been removed, the possible recovery of the Au/P3HT surface has been confirmed after 10 minutes, as shown in **Figure 4.12(d)**. The interaction and recovery mechanism of the ammonia gas over an Au-doped P3HT sensing surface is clearly illustrated in **Figure 4.12(d)** over time.

4.5 Conclusion

The current work aims to fabricate a low voltage operated, cost-efficient, high-performance solution-processed organic TFT for highly sensitive ammonia gas at RT (25 °C) utilizing Au/P3HT as a sensing layer. In the present work, a bilayer dielectric (TiO_2/HfO_2) has been synthesized using a low-cost spin coating method to fabricate a low-voltage operated OTFT. The fabricated dialectic passes with low RMS surface roughness of 0.915 nm, a high band gap of 5.6 eV, a high dielectric constant of ~ 42, and a high dielectric capacitance of 0.926 μF/cm^2, and low leakage current density of ~1 μA/cm^2. The incorporation of TiO_2 and HfO_2 used in bilayer dielectric combines the advantages of both single layers in terms of high oxide capacitance (TiO_2 k value 60-80) and low leakage current density (HfO_2 band gap 5.8 eV), making it suitable for high-performance organic TFT. The OSC was deposited by a low-cost, minimal-wastage solution processed FTM method. The obtained FTM-deposited Au-doped

P3HT OSC film has an almost uniform thickness of 30±5 nm and has been utilized for ammonia gas sensing at RT (25 °C). The fabricated solution-processed organic TFT has a high sensing response of 55%, and a quick response/recovery time of 6/17 sec., respectively, at 5 ppm ammonia gas. The present study briefly explains to fabricate a high-k bilayer dielectric-based, low voltage operated solution processed OTFT device for ammonia gas sensing at RT.